Journal of Laser Applications

Pulse-to-pulse evolution of optical properties in ultrafast laser micro-processing of polymers

Cite as: J. Laser Appl. **33**, 012020 (2021); https://doi.org/10.2351/7.0000306
Submitted: 30 November 2020 . Accepted: 30 November 2020 . Published Online: 23 December 2020

Arifur Rahaman, Xinpeng Du, Boyang Zhou, Aravinda Kar, and Xiaoming Yu

Journal of Laser Applications ARTICLE scitation.org/journal/jla

Pulse-to-pulse evolution of optical properties in ultrafast laser micro-processing of polymers

Cite as: J. Laser Appl. 33, 012020 (2021); doi: 10.2351/7.0000306
Submitted: 30 November 2020 · Accepted: 30 November 2020 ·
Published Online: 23 December 2020

Arifur Rahaman, Xinpeng Du, Boyang Zhou, Aravinda Kar, and Xiaoming Yu[a)]

AFFILIATIONS

CREOL, The College of Optics and Photonics, University of Central Florida, Orlando, Florida 32816

Note: Paper published as part of the special topic on Proceedings of the International Congress of Applications of Lasers & Electro-Optics 2020.

[a)]**Electronic mail:** yux@creol.ucf.edu

ABSTRACT

Polymers were one of the first materials to be processed by ultrafast lasers. However, the nature of absorption for near-infrared laser beams is not fully understood, and therefore it remains challenging to process polymeric materials with high energy efficiency. In this study, the pulse-to-pulse evolution of optical properties (reflectance, transmittance, and absorptance) of polypropylene (PP), which is an important polymeric material widely used in many industrial applications, is determined by performing time-resolved measurements for a wide range of pulse energies. The goal is to differentiate between linear and nonlinear absorption in different laser-matter interaction regimes and select the processing condition that yields the highest energy efficiency. The experiment is performed by recording the reflection and transmission of each laser pulse in an ellipsoidal mirror-based setup, which enables the collection of scattering reflection with nearly full coverage. Absorption is calculated from the experimental data, and a model consisting of linear and nonlinear absorption is used to analyze the results. It is found that PP undergoes a dramatic morphological change from pulse to pulse, which is accompanied by changes in optical properties, that is, the tuning of the laser condition to fully utilize the laser energy. Their results could help increase energy efficiency in ultrashort-pulsed laser processing of polymers toward the high-throughput operation.

Key words: Polymer processing, Ultrafast laser, Polymers, Optical properties, Absorption, time-resolved measurement

I. INTRODUCTION

Recent advances in ultrafast laser technology facilitate researchers to focus on understanding the physical process of ultrashort pulse interaction with materials and its applications for high-precision material processing in scientific and industrial applications.[1–4] Ultrafast lasers have been used in various types of material processing including laser cutting,[5] drilling,[6] polishing,[7] cleaning,[8] and micro/nanomachining.[9] Ultrafast lasers produce minimal thermal damage to the material, which makes these lasers attractive for processing polymeric materials, which typically have a low decomposition temperature.[10] The interest in the ultrafast laser micro-processing of polymeric materials remains strong due to the high demand for using these materials in scientific and industrial applications.[11–16] However, material processing with ultrafast lasers is quite complicated due to the dynamic behavior of laser–matter interaction, and there are pulse-to-pulse variations of the interaction mechanism. Therefore, ultrafast laser microprocessing of polymeric materials with high precision and control is still challenging.[17,18]

Laser processing with multiple ultrafast laser pulses has been already discussed in various articles.[19–22] Li *et al.*[21] observed the morphological evolution and dynamics of femtosecond laser ablation of bulk polymethylmethacrylate (PMMA) irradiated with a pair of pulses with experimental and numerical studies. Hu[23] showed that a second delayed pulse causes an increase in the ion emission from Si and enhanced absorption of the second pulse was suggested as the reason for increased ion emission. Researchers also found that the material response and the ablation process have a significant dependence on the delay between the pulses.[24] Most of the studies were performed with metals and dielectrics by using the pump-probe technique. For polymers, the understanding of fundamental mechanisms involved is still lacking, especially in the near-infrared (NIR) wavelength. In addition, determining pulse-to-pulse interaction

mechanisms, especially optical properties such as reflectance, transmittance, and absorption, is crucial for selecting laser-processing parameters to maximize energy efficiency for industrial applications.

In this study, the pulse-to-pulse evolution of optical properties, such as reflectance, transmittance, and absorptance, is determined by performing time-resolved measurements in ultrafast laser interaction with polypropylene. The time-resolved measurement is performed by using an ellipsoidal mirror-based system, which can collect both specular and diffusive reflection from the irradiated sample. The measurements are carried out for each of the pulses in a double-pulse configuration for a wide range of fluences, and the measurement of optical properties is compared with observed damage morphology. The absorption is explained with a model that includes both linear and nonlinear mechanisms.

II. EXPERIMENTAL SETUP

The experimental setup is shown in Fig. 1. A Yb: KGW (Yb-doped potassium gadolinium tungstate) femtosecond laser from Light Conversion at a central wavelength of 1030 nm is used as the laser source. It delivers 170 fs to 10 ps ultrashort pulses with the maximum pulse energy of 1 mJ and repetition rate tunable from a single pulse to 1 MHz. The output beam with a diameter of 4 mm is expanded by a beam expander to 10 mm in diameter, and the laser power is controlled with a variable neutral density (ND) filter. The laser beam is split into two arms, one as the reference arm, which has 6.5% of the incident light and is used to determine the incident laser pulse energy, and the other as the source arm, which is focused onto the sample with a lens of 250 mm focal length. The diameter of the spot size is measured to be 36.8 μm at the $1/e^2$-point.

A 1-GHz oscilloscope (Tektronics, MD03104), which is not shown in Fig. 1, and three photodiodes (PD 1–3, Thorlabs, FDS100) are used for data acquisition. Commercially available transparent PP sheets (PP301440, Goodfellow) of thickness 450 μm are used in this experiment as samples, which are placed on the top of a fixture (Fig. 1, inset) and are close to the first focus of an ellipsoidal mirror (E180, Optiforms). An ND filter with a diameter of 12.5 mm and PD 3 is placed in the fixture. To capture the reflected light (both specular and diffusive reflection) from the sample,[25,26] an ellipsoidal mirror (E180, Optiforms) is used, and the reflected light is detected by PD 2 at the second focus of the ellipsoidal mirror. The procedure to place PD 2 at the second focus of the ellipsoidal mirror has been discussed elsewhere.[27] To ensure a fresh surface for each laser shot, a 3D stage is used to move the sample for irradiating with different pulse energies. The sample is irradiated with a total of two pulses and time-resolved optical properties, such as reflectance and transmittance, are measured experimentally. PD 2 is used to measure the reflectance light, and PD 3 is used for the transmittance light. Figure 1 also shows the damage profile for single pulse damage at the upper left and double-pulse damage in the upper right. As will be discussed next, a single pulse creates swelling and the double pulses create a crater.

In this study, transparent polypropylene (PP301440, Goodfellow, which is mostly transparent, around 91% of visible light) samples are used. Absorption of polymer is dependent on additives and impurities, and therefore the secondary ion mass spectroscopy (SIMS) has been performed, The SIMS measurement confirms that the transparent PP sample used in this experiment is almost pure.

According to the manufacturer, this sample is semicrystalline, white, semiopaque commodity thermoplastic. It is a linear

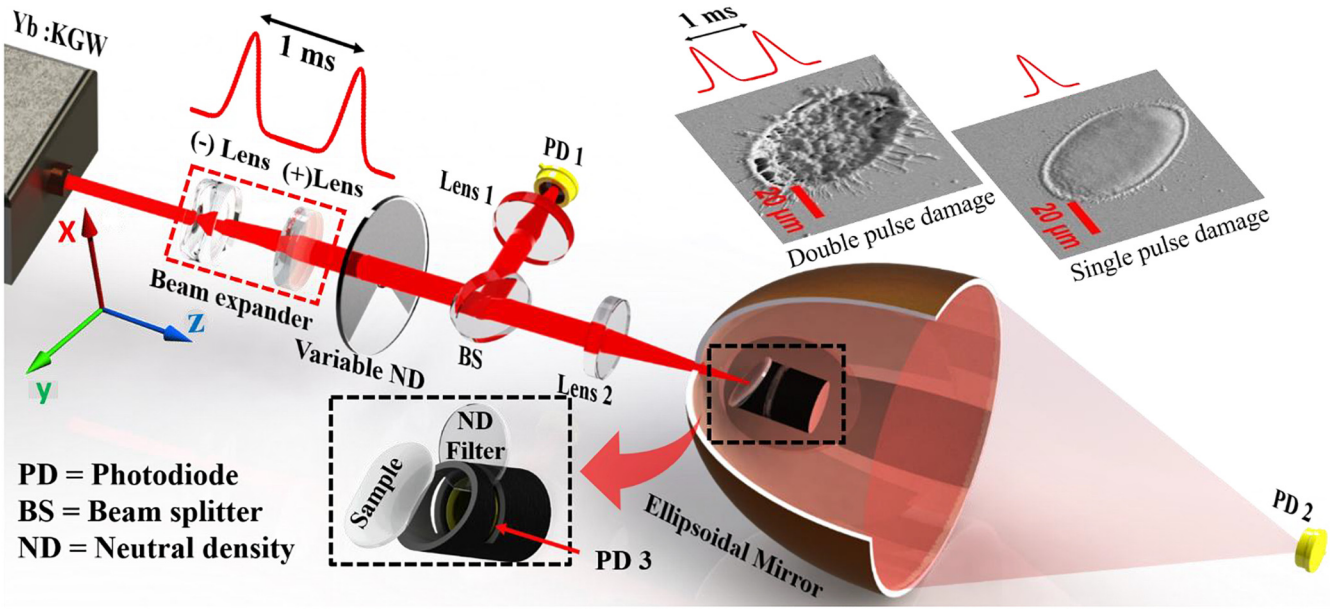

FIG. 1. Experimental setup for measuring the optical properties of ultrafast laser interaction with transparent PP.

polyolefin that can be compared in many ways to high density polyethylene and that is manufactured in a very similar way.

III. EXPERIMENTAL RESULTS

The measurements of optical properties for the two pulses are performed with a wide range of peak fluences, from well below to well above the damage threshold. The sample is irradiated with a pair of identical pulses with a delay of 1 ms to avoid the effects that happened within a shorter time duration. Both pulses are focused at the same spot on the sample, and the surface of the sample is tilted with an incident angle of 17° to reduce backscattering through the entrance hole of the ellipsoidal mirror.

Figure 2 shows the damage on the surface of the transparent PP sample and the corresponding damage profiles for both single pulse and a pair of pulses. The left side of Fig. 2 shows damages irradiated with a single pulse. Damages A, B, C, and D are irradiated with the single pulse energies of 20, 30, 50, and 100 μJ, respectively, that correspond to the peak fluences of 0.94, 3.76, 5.64, and 18.8 J/cm^2, respectively. The 2D profilometer (Dektak, Bruker) measurements are performed to confirm the damage profiles, which are shown next to the SEM (scanning electronic microscopy) image of the damage profile. It is obvious from both SEM image and profilometer measurements that single-pulse irradiation with fluences 3.76, 5.64, 9.4, and 18.8 J/cm^2 creates dome-shaped swelling. The maximum height of the dome is around 1.75 μm from the profilometer measurement. Similarly, the right-hand side of Fig. 2 shows the damage with the double-pulse irradiation. Damages E, F, G, and H are irradiated with an additional pulse with the same fluences as the respective single-pulse damage. The profilometer measurements are shown next to the damages. For the double-pulse case, craters are observed at the surface of the sample and the maximum depth of the crater is found to be 5.7 μm.

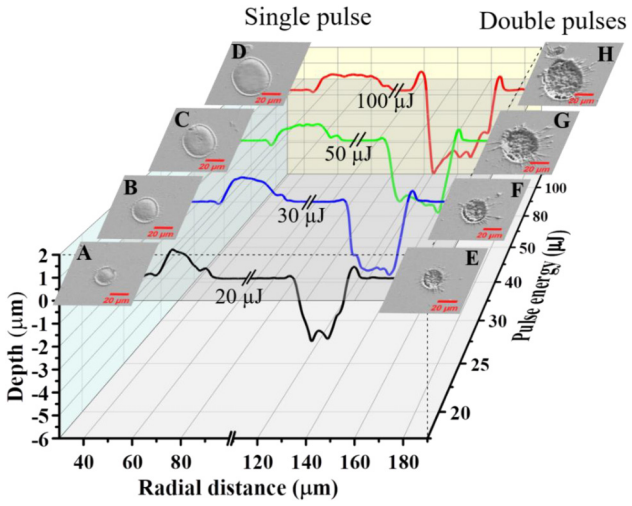

FIG. 2. SEM pictures and z-profile of surface damages obtained after single (left) or double (right) pulse laser irradiation for different pulse energies ranging from 20 to 100 μJ. The damage profiles are shown beside each of the damages.

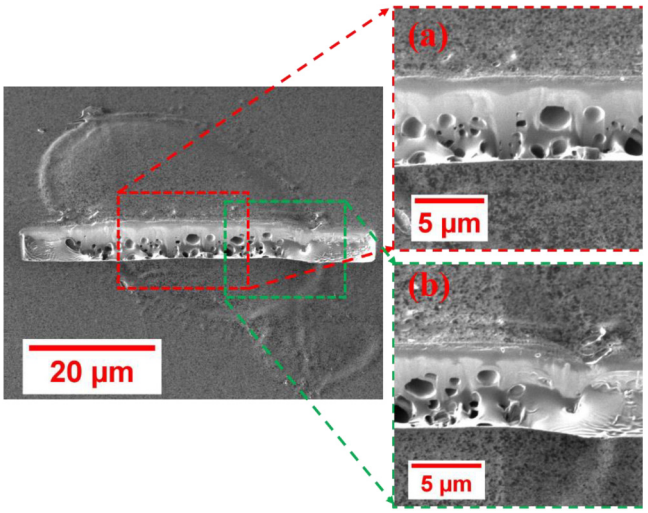

FIG. 3. Cross-sectional analysis of transparent PP sample with focused ion beam (FIB) milling, which is irradiated at pulse energy 80 μJ and pulse duration 167 fs.

It is found that single-pulse irradiation creates voids below the surface of the sample, as is shown in Fig. 3, which shows the evidence of void formation near to the surface. The cross-sectional analysis of the irradiated sample is performed with a focused ion beam (FIB) milling, where the sample is irradiated with a pulse energy of 80 μJ. The inset (a) in Fig. 3 shows the center part of the irradiated region, where the formation of the voids is denser than the periphery as the intensity of the laser is higher at the center. The diameter of the voids is found to be increasing with pulse energies, and the diameter of the voids is found to be 0.2–3 μm corresponding to the pulse energy 12.5–100 μJ. The inset (b) in Fig. 3 shows a comparison between the irradiated region, where the void formation is found near to the surface, and the non-irradiated region, where no void is observed near to the surface. The instantaneous heating[27,28] and expansion[29,30] occur due to the ultrashort pulse irradiation on the surface of the polymeric material. Micro/nano splashes are observed at the surface of the sample due to the localized melting and explosive boiling and a two-phase liquid–gas mixture develops after thermalization of the laser pulse in the polymeric sample in the ps time scale. Then, material ejection and resolidification take place in the ns time scale[30,31] due to hydrodynamics expansion, which is the reason for the formation of micro/nanovoids as well as dome-shaped swelling.[32,33]

Figure 5 shows the total reflectance (specular and diffusive), R, transmittance, T, and absorptance, A, as a function of peak fluence for first pulse and second pulse in the double-pulse case. To determine R and T, an integrated area at FWHM (full width at half maximum) of the oscilloscope traces for the PD signals for reflection and transmission is used with proper scaling based on the ND attenuation and more discussion on determining R, T, and A can be found elsewhere.[27] In this study, it is observed that the threshold peak fluence, which is defined from material surface measurements, for surface damage of the transparent PP sample is 0.94 J/cm^2 with

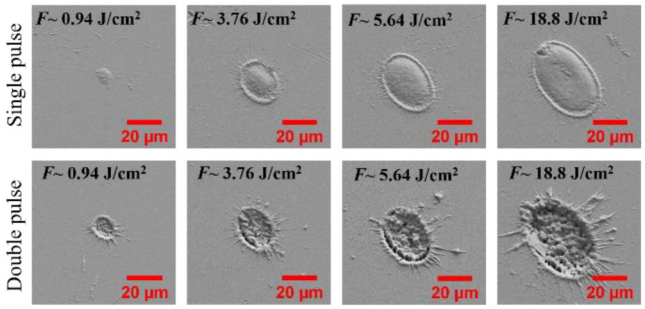

FIG. 4. Surface damage with a single pulse (top) and double pulse (bottom) with different peak fluences.

single pulse irradiation. Since the material surface does not undergo any surface modification <0.94 J/cm^2, the reflectance and transmittance remain constant up to the peak fluence 0.94 J/cm^2 for the first pulse in the case of multiple pulse irradiation. Therefore, this constant peak fluence/intensity region is defined as the "linear absorption region" for single pulse absorption. Similarly, the absorptance remains constant for the peak fluence of <0.94 J/cm^2 as it is determined from the reflectance and transmittance, $A = 1 - R - T$. The transmittance and reflectance start to drop after the peak fluence reaches the threshold peak fluence due to nonlinear absorption with high intensity, which will be discussed in Sec. IV.

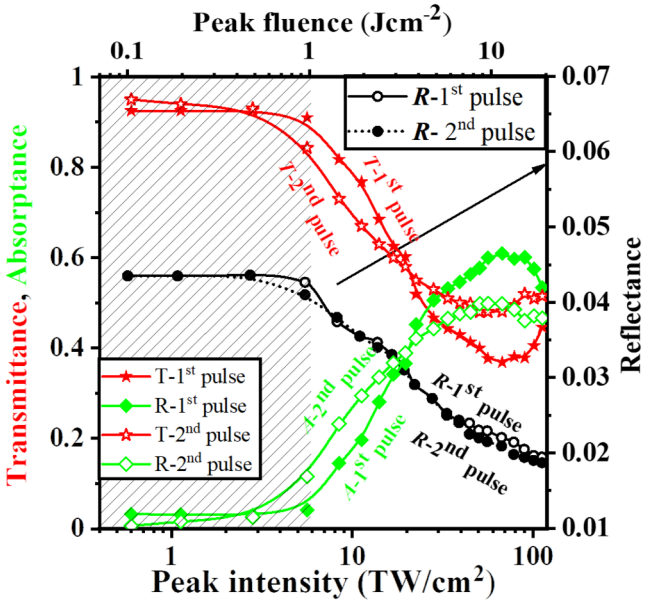

FIG. 5. Reflectance (R), transmittance (T), and absorptance (A) as a function of peak fluence for the first pulse (circular data point) and the second pulse (star data points) in double pulse case with the delay 1 ms (uncertainty of this measurement is about ±0.012), where the duration in this case is 167 fs.

It can be seen from Fig. 4 that the second irradiated pulse is not behaving exactly the same as the first irradiated pulse due to the modification that happened in the surface and inside the sample. The reflectance for the first pulse and the second pulse looks quite similar except at very high peak fluences, where the surface morphology has changed, as can be seen, from Figs. 2 and 4.

It can be seen from Fig. 5 that the transmittance for the first pulse and the second pulse is distinct from each other except some crossing points. The formation of micro/nanovoids with the first pulse could be the reason for the changed transmission inside the material for the second pulse. For low pulse energy, the size of the voids is smaller inside the material; therefore, the transmitted light is attenuated more inside the material, and the transmission gets lower for the second pulse. However, the diameter of the voids increases with pulse energy, and a more hollow region is formed inside the material, which allows transmitting more light for higher fluence for the case of the second laser pulse.

IV. THEORETICAL ANALYSIS

Ultrafast lasers have been used for various high precision polymer processing, but several fundamental questions are still not clear. Therefore, it is required to understand those fundamental questions including the relative significance of different linear and nonlinear absorption regimes and interaction mechanisms with different kinds of materials for high precision material processing. For polymeric materials, which have a wide bandgap, the absorption mechanism has the contribution of both linear (single-photon) and nonlinear (multi-photon) processes.[27,34] However, the absorption mechanism for polymer processing with the NIR wavelength is happened due to vibrational overtone or combination absorption.[35] The equation that describes the attenuation of the spatial and radial intensity, $I(r, z, t)$ of the ultrafast laser, which is passing through the material undergoing single-photon, two-photon or two-steps, or three-photon or three-steps absorption is given by

$$\frac{dI(r_i, z_i, t)}{dz_i} = -\alpha_1 I(r_i, z_i, t) - \alpha_2 I^2(r_i, z_i, t) - \alpha_3 I^3(r_i, z_i, t), \quad (1)$$

where α_1, α_2, and α_3 are linear and nonlinear absorption coefficients for single-photon (linear), two-photon or two-steps (nonlinear), and three-photon or three-steps (nonlinear), respectively. The electric field enhancement[36] at the back surface inside the material is not considered in Eq. (1). The effect of this enhancement is, however, negligible when the absorption coefficient is very small, and therefore Eq. (1) can be applied to weakly absorbing media. In addition, Eq. (1) would be applicable to optically thick material, i.e., when the geometrical thickness of the material is much larger than the coherence length of the laser inside the material.[37–39] The wavelength shifts from $\Delta\lambda = 10$ to 30 nm due to self-phase modulation (SPM) for the intensities considered in this study. Thus, the coherence length, $l_c = (\lambda_o/n)^2/\Delta\lambda$, varies from 71.2 to 23.7 μm corresponding to $\Delta\lambda = 10$ and 30 nm, respectively, where n is taken to be the linear refractive index, 1.49. Since these values of l_c are much smaller than the sample thickness, $L = 450\,\mu$m, the sample of this study is considered to be optically thick.

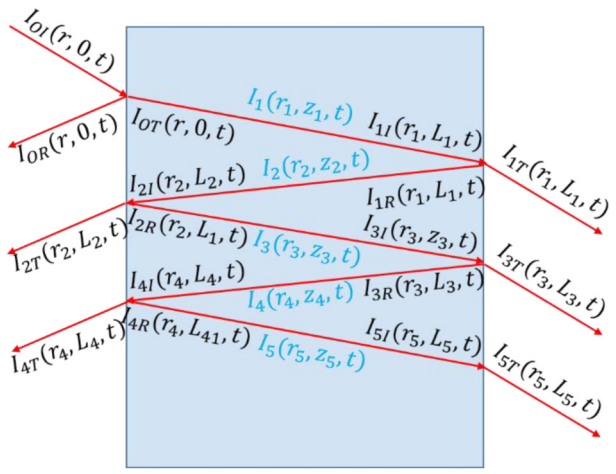

FIG. 6. The multiple reflection is considered an inclined laser beam that is irradiated on the sample.

The analytical solution of the above differential equation after passing through the material can be expressed as

$$I_{iI}(r_i, z_i, t) = \frac{1}{3a_i(r_i, z_i, t)}\left(Q_i(r_i, z_i, t) + \frac{\Delta_{oi}(r_i, z_i, t)}{Q_i(r_i, z_i, t)} - b_i(r_i, z_i, t)\right), \tag{2}$$

where $I_{iI}(r_i, L_i, t)$ is the incident intensity at the different interfaces except for the first incident point, which is shown in Fig. 6. All the variables in the above equation are defined in the Appendix.

The total transmitted intensity at the exit side of the sample is given by

$$I_T(r, z, t) = \sum_{m=0}^{\infty} I_{(2m+1)T}(r_{(2m+1)}, L_{(2m+1)}, t). \tag{3}$$

Here, the transmitted light at each of the points is $I_{iT}(r_i, L_i, t)$. The total reflected light intensity at the exit side of the sample is given by

$$I_R(r, z, t) = I_{OR}(r, 0, t) + \sum_{m=1}^{\infty} I_{(2m)T}(r_{(2m)}, L_{(2m)}, t). \tag{4}$$

The transmittance, T, and reflectance, R, of the ultrafast laser pulse through the PP sample can be found from the above solution in Eq. (2), which can be expressed as

$$T = \frac{I_T(r, z, t)}{I_{OI}(r, 0, t)}, \qquad R = \frac{I_R(r, z, t)}{I_{OI}(r, 0, t)}. \tag{5}$$

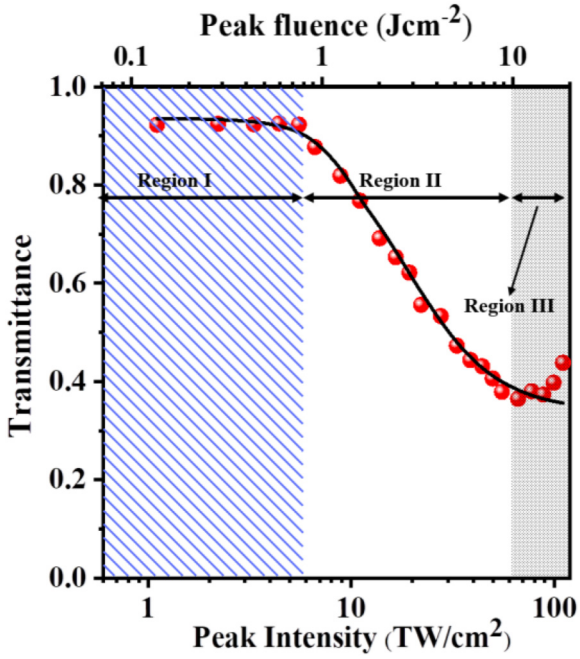

FIG. 7. Fitting of the experimental results of 167 fs for a transparent PP sample. The laser intensity used in this experiment can be divided into three regions (regions I, II, and III). Note that the pulse duration in this case is 167 fs.

Figure 7 shows the experimental results of transmittance fitted with theoretical calculation, where the transmittance is divided into three fluence/intensity regions. Region I represents the linear absorption region, and regions II and III represent the nonlinear region as defined in Sec. III. It can be seen that the transmittance remains constant until the fluence/intensity reaches the damage threshold peak fluence/intensity, where the damage threshold peak fluence is found to be 0.94 J/cm^2. The transmittance starts to decrease after the damage threshold peak fluence as shown in Fig. 5, which indicates nonlinear absorption. The transmission keeps decreasing until the peak fluence reaches 10 J/cm^2. Note that the absorptance of the sample increases in region II as the transmittance decreases.

In this study, the linear and nonlinear absorption coefficients are determined from the fitting results of the experimental data of T and A with the theoretical calculation of Eq. (5) for different pulse durations, i.e., 167, 371, and 710 fs, which is shown in Fig. 8. The average value of the linear (single-photon) absorption coefficient for three pulse durations (i.e., 167, 371, and 710 fs) is found to be $\alpha_1 = (110.45 \pm 3)\ \mathrm{m}^{-1}$, which agrees with the experimental value determined from the linear spectroscopic measurement for the thickness of the transparent sample, $L = 450\ \mu\mathrm{m}$. The linear refractive index of this transparent polypropylene sample is 1.49.

The average (from three pulse durations) value of nonlinear absorption coefficients for two-photon or two-steps absorption and the three-photon or three-steps absorption is found to be

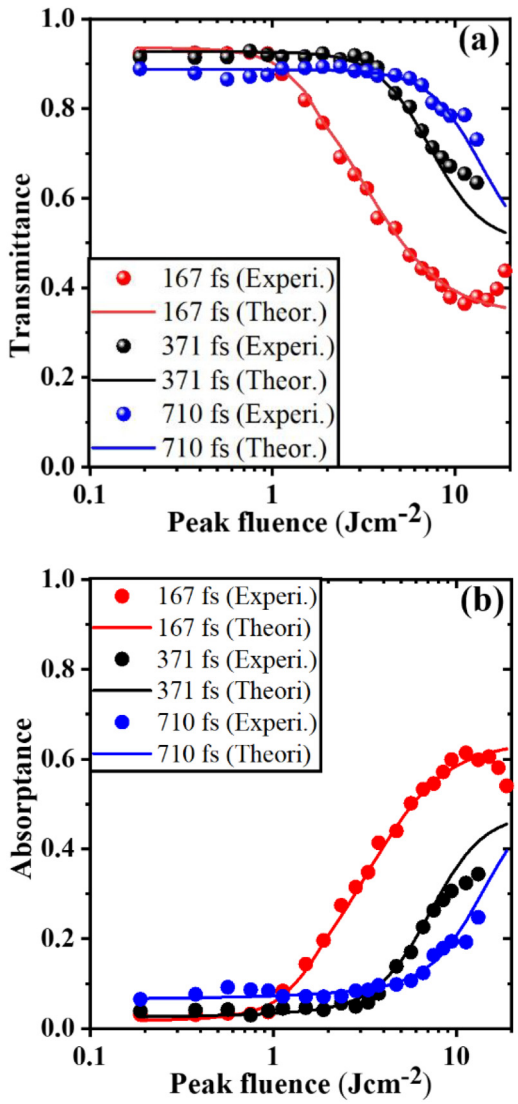

FIG. 8. The experimental results of (a) transmittance and (b) absorptance ($A = 1 - R - T$) for different pulse durations (i.e., 167, 371, and 710 fs are fitted with the theoretical calculation).

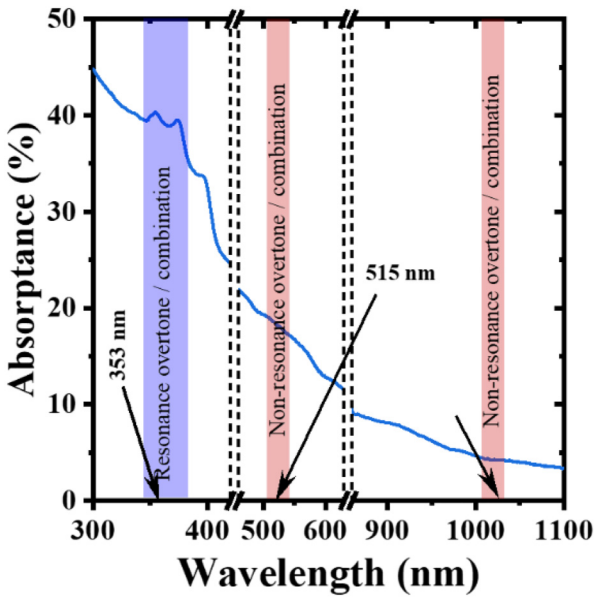

FIG. 9. Absorptance, A, of transparent PP sample is determined from the linear spectroscopic measurement.

$\alpha_2 = (8.01 \pm 2.15) \times 10^{-13}$ m W^{-1} and $\alpha_3 = (3.21 \pm 1.0) \times 10^{-29}$ m^3 W^{-2}, respectively, from the fitting result, and those values are consistent with the previously reported value for the polymeric materials.[40,41] The average (from three pulse duration) value of nonlinear refractive indexes is found to be $n_2 = (3.22 \pm 1.15) \times 10^{-20}$ m^2 W^{-1} and $n_3 = (2.64 \pm 1) \times 10^{-37}$ m^4 W^{-2}. This study suggests that the non-resonance vibrational overtone or combination absorption happened at 1030 and 515 nm, and resonance overtone or combination absorption happened at 353 nm, which is shown in Fig. 9. The fundamental wavelength used in this study is 1030 nm; therefore, the third-harmonic of the fundamental wavelength could be around 343 nm. However, the absorption peak from linear spectroscopic measurement is found to be at 353 and 373 nm.

When a high-intensity laser pulse propagates through a nonlinear medium, an ultrashort pulse accumulates the temporal phase as it propagates, which is known as SPM, which is a nonlinear Kerr-like phenomenon due to the nonlinear refractive index change inside the medium.[42,43] Therefore, the wavelength shifting due to SPM phenomena can be written as

$$\lambda(t) - \lambda_o = \lambda_o \left(\frac{n_2(dI(t)/dt) + 2n_3 I(t)(dI(t)/dt)}{(c/z) - n_2(dI(t)/dt) - 2n_3 I(t)(dI(t)/dt)} \right). \quad (6)$$

The maximum wavelength shifting corresponding to the maximum peak intensity 106.1 TW/cm^2 is found to be around ± 30 nm, which covers both peaks at 353 and 373 nm. Therefore, three-steps or three-photon absorption is suggested to have happened through the vibrational overtone absorption mechanism by shifting wavelength at a very high intensity of the laser beam.

V. CONCLUSIONS

In summary, the pulse-to-pulse evaluation of optical properties of polypropylene in ultrafast laser interaction is determined by performing time-resolved measurement for the multiple pulse configuration for a wide range of intensities from below to well above the damage threshold. The measurements of the optical properties show a strong correlation with damage morphology. The experimental data are explained with a model that includes the linear and nonlinear absorption mechanism and the absorption coefficients

are determined. Our results could be useful for optimizing parameters for the ultrafast laser processing of polymers.

ACKNOWLEDGMENTS

Financial support from Elsner Engineering Works is appreciated.

APPENDIX

After performing integration, Eq. (1) can be written as a general cubic equation as

$$a_i I^3(r_i, z_i, t) + b_i I^2(r_i, z_i, t) + c_i I(r_i, z_i, t) + d_i = 0, \tag{A1}$$

where a_i, b_i, c_i, and d_i can be expressed as

$$\begin{aligned} a_i(r_i, z_i, t) &= \frac{2\alpha_3}{\alpha_1} - \frac{2\alpha_3^2}{\alpha_1^2} k_i(r_i, z_i, t), \\ b_i(r_i, z_i, t) &= N - \left(\frac{\alpha_2\alpha_3}{\alpha_1^2} + \frac{\alpha_3 M}{\alpha_1}\right) k_i(r_i, z_i, t), \\ c_i(r_i, z_i, t) &= -\left(\frac{2\alpha_3}{\alpha_1} + \frac{\alpha_2 M}{\alpha_1}\right) k_i(r_i, z_i, t), \\ d_i(r_i, z_i, t) &= -M k_i(r_i, z_i, t). \end{aligned} \tag{A2}$$

Here, M, N, and k are

$$\begin{aligned} M &= \frac{\alpha_2}{\alpha_1} - \frac{\alpha_2}{\alpha_1}\sqrt{1 - \frac{4\alpha_1\alpha_3}{\alpha_1^2}}, \\ N &= \frac{\alpha_2}{\alpha_1} + \frac{\alpha_2}{\alpha_1}\sqrt{1 - \frac{4\alpha_1\alpha_3}{\alpha_1^2}}, \end{aligned} \tag{A3}$$

$$k_i(r_i, z_i, t) = \frac{((2\alpha_3/\alpha_1)I^3(r_i, z_i, t) + NI^2(r_i, z_i, t))e^{-2\alpha_1 z_i}}{(2\alpha_3/\alpha_1)I(r_i, z_i, t) + (2\alpha_3\alpha_2/\alpha_1^2)I^2(r_i, z_i, t) + (2\alpha_3^2/\alpha_1^2)I^3(r_i, z_i, t) + (\alpha_2 M/\alpha_1)I(r_i, z_i, t) + (\alpha_3 M/\alpha_1)I^2((r_i, z_i, t)}.$$

Therefore, the solution of Eq. (A1) can be expressed for the incoming beam at every interface except the first incident point as

$$I_{iI}(r_i, L_i, t) = \frac{1}{3a_i(r_i, z_i, t)}\left(Q_i(r_i, z_i, t) + \frac{\Delta_{oi}(r_i, z_i, t)}{Q_i(r_i, z_i, t)} - b_i(r_i, z_i, t)\right). \tag{A4}$$

The other two roots of the cubic equation are ignored in this study as it is not applicable for our case. Here, $Q_i(r_i, z_i, t)$ and $\Delta_{oi}(r_i, z_i, t)$ in Eq. (A4) can be expressed as

$$Q_i(r_i, z_i, t) = \sqrt[3]{\frac{\sqrt{\Delta_{1i}^2(r_i, z_i, t) - 4\Delta_{oi}^3(r_i, z_i, t)} - \Delta_{1i}(r_i, z_i, t)}{2}},$$

$$\Delta_{oi}(r_i, z_i, t) = b_i^2(r_i, z_i, t) - 3a_i(r_i, z_i, t)c_i(r_i, z_i, t),$$

$$\Delta_{1i}(r_i, z_i, t) = 2b_i^2(r_i, z_i, t) - 9a_i(r_i, z_i, t) + 27a_i^2(r_i, z_i, t)d_i(r_i, z_i, t)\ .$$

Here, the transmitted light at each of the points $I_{iT}(r_i, L_i, t)$ is related to $I_{iI}(r_i, L_i, t)$ as

$$\begin{aligned} I_{iT}(r_i, L_i, t) &= T_{ie}(I_{iI})I_{iI}(r_i, L_i, t), \\ I_{0T}(r, 0, t) &= T_{0I}(I_{0I})I_{0I}(r, 0, t). \end{aligned} \tag{A5}$$

Here, $T_{OI}(I_{OI})$ and $T_{ie}(I_{iI})$ are the transmission coefficient at the first incoming point and all others can be expressed as

$$\begin{aligned} T_{OI}(I_{0I}) &= \frac{4(n_1 + n_2 I_{oI} + n_3 I_{OI}^2)}{((n_1 + n_2 I_{oI} + n_3 I_{OI}^2)^2 + 1)^2 + \kappa^2}, \\ T_{ie}(I_{iI}) &= \frac{4(n_1 + n_2 I_{iI} + n_3 I_{iI}^2)}{((n_1 + n_2 I_{iI} + n_3 I_{iI}^2)^2 + 1)^2 + \kappa^2}, \\ \kappa &= \frac{\lambda(\alpha_1 + \alpha_2 I_{iI} + \alpha_3 I_{iI}^2)}{4\pi}, \end{aligned} \tag{A6}$$

where, n_1, n_2, and n_3 are the real parts of the linear, nonlinear third-order, and nonlinear fifth-order refractive index, respectively, and κ is the imaginary part of the nonlinear refractive index.

Here, the reflected light at each of the points $I_{iR}(r_i, L_i, t)$ is related to $I_{iI}(r_i, L_i, t)$ as

$$\begin{aligned} I_{iR}(r_i, L_i, t) &= R_{ie}(I_{iI})I_{iI}(r_i, L_i, t), \\ I_{0R}(r, 0, t) &= R_{0I}(I_{0I})I_{0I}(r, 0, t). \end{aligned} \tag{A7}$$

Here, $R_{OI}(I_{OI})$ and $R_{ie}(I_{iI})$ are the transmission coefficient at the first incoming point and all other can be expressed as

$$R_{OI}(I_{0I}) = \frac{((n_1 + n_2 I_{oI} + n_3 I_{OI}^2)^2 - 1)^2 + \kappa^2}{((n_1 + n_2 I_{oI} + n_3 I_{OI}^2)^2 + 1)^2 + \kappa^2},$$
$$R_{ie}(I_{ie}) = \frac{((n_1 + n_2 I_{iI} + n_3 I_{iI}^2)^2 - 1)^2 + \kappa^2}{((n_1 + n_2 I_{iI} + n_3 I_{iI}^2)^2 + 1)^2 + \kappa^2}. \quad \text{(A8)}$$

REFERENCES

[1]K. Sugioka and Y. Cheng, "Ultrafast lasers—Reliable tools for advanced materials processing," Light Sci. Appl. **3**, 1–12 (2014).
[2]W. Sibbett, A. A. Lagatsky, and C. T. A. Brown, "The development and application of femtosecond laser systems," Opt. Express **20**, 6989–7001 (2012).
[3]K. C. Phillips, H. H. Gandhi, E. Mazur, and S. K. Sundaram, "Ultrafast laser processing of materials: A review," Adv. Opt. Photonics **7**, 684–712 (2015).
[4]Y. Acosta, Q. Zhang, A. Rahaman, H. Ouellet, C. Xiao, J. Sun, and C. Li, "Imaging cytosolic translocation of mycobacteria with two-photon fluorescence," Bio. Opt. Express **5**, 3990–4001 (2014).
[5]A. N. Fuchs, M. Schoeberl, J. Tremmer, and M. F. Zaeh, "Laser cutting of carbon fiber fabrics," Phys. Procedia **41**, 372–380 (2013).
[6]X. Zhao and Y. C. Shin, "Femtosecond laser drilling of high - aspect ratio microchannels in glass," Appl. Phys. A **104**, 713–719 (2011).
[7]L. L. Taylor, J. Xu, M. Pomerantz, T. R. Smith, J. C. Lambropoulos, and J. Qiao, "Femtosecond laser polishing germanium," Opt. Express **9**, 4165–4177 (2019).
[8]T. Ersoy, T. Tunay, M. Uğuryol, G. Mavili, and S. Akturk, "Femtosecond laser cleaning of historical paper with sizing," J. Cult. Herit. **15**, 258–265 (2014).
[9]R. R. Gattass and E. Mazur, "Femtosecond laser micromachining in transparent materials," Nat. Photonics **2**, 219–225 (2008).
[10]Y. K. Godovsky, *Thermophysical Properties of Polymers* (Springer, New York, 1992).
[11]A. Shibata, S. Yada, and M. Terakawa, "Biodegradability of poly (lactic-co-glycolic acid) after femtosecond laser," Sci. Rep. **6**, 27884 (2016).
[12]M. Terakawa, "Femtosecond laser processing of biodegradable polymers," Appl. Sci. **8**, 1123–1135 (2018).
[13]A. Rahaman, A. Kar, and X. Yu, "Thermal effects of ultrafast laser interaction with polypropylene," Opt. Express **27**, 5764–5783 (2019).
[14]A. Rahaman, X. Du, B. Zhou, H. Cheng, A. Kar, and X. Yu, "Absorption and temperature distribution during ultrafast laser micro-cutting of polymeric materials," J. Laser Appl. **32**, 022044 (2020).
[15]B. Zhou, A. Rahaman, X. Du, H. Cheng, A. Kar, and X. Yu, "Laser processing of dielectrics using spatiotemporally tuned ultrashort pulses," J. Laser Appl. **32**, 022041 (2020).
[16]B. Zhou, A. Rahaman, X. Du, H. Cheng, Y. Chai, A. Kar, and X. Yu, Proc. SPIE **10906**, 109061R (2019).
[17]K. Sugioka, "Progress in ultrafast laser processing and future prospects," Nanophotonics **6**, 393–413 (2017).
[18]M. V. Shugaev, C. Wu, O. Armbruster, A. Naghilou, N. Brouwer, D. S. Ivanov, T. J. Y. Derrien, N. M. Bulgakova, W. Kautek, B. Rethfeld, and L. V. Zhigilei, "Fundamentals of ultrafast laser-interaction," MRS Bull. **41**, 960–968 (2016).
[19]T. Donnelly, J. G. Lunney, S. Anoruso, R. Bruzzese, X. Wang, and X. Ni, "Double pulse ultrafast laser ablation on nickel in a vacuum," J. Appl. Phys. **106**, 013304 (2009).
[20]S. Amoruso, R. Bruzzese, and X. Wang, "Plume composition control in double pulse ultrafast laser ablation of metals," Appl. Phys. Lett. **95**, 251501 (2009).
[21]M. Li, S. Menon, J. P. Nibarger, and G. N. Gibson, "Ultrafast electron dynamics in femtosecond optical breakdown of dielectrics," Phys. Rev. Lett. **82**, 2394–2397 (1999).
[22]F. Baset, K. Popov, A. Villafranca, A. M. Alshehri, J. M. Guay, L. Ramunno, and V. R. Bhardwaj, "Nanopillar formation from two-shot femtosecond laser ablation of poly-methyl methacrylate," Appl. Surf. Sci. **357**, 273–281 (2015).
[23]Z. Hu, "Mechanism for the ablation of Si<111> with pairs of ultrashort laser pulses," Appl. Phys. Lett. **90**, 131910 (2007).
[24]M. E. Povarnitsyn, T. E. Itina, K. V. Khishchenko, and P. R. Levashov, "Suppression of ablation in femtosecond double-pulse experiments," Phys. Rev. Lett. **103**, 195002 (2009).
[25]A. Y. Vorobyev and C. Guo, "Reflection of femtosecond laser light in multi-pulse ablation of metals," J. Appl. Phys. **110**, 043102 (2011).
[26]O. Benavides, O. Lebedeva, and V. Golikov, "Reflection of nanosecond Nd: YAG laser pulses in ablation of metals," Opt. Express **19**, 21842 (2011).
[27]A. Rahaman, A. Kar, and X. Yu, "Time-resolved measurements of optical properties in ultrafast laser interaction with polypropylene," Opt. Express **28**, 2640–2648 (2020).
[28]F. Baset, A. Villafranca, J. M. Guay, and R. Bhardwaj, "Femtosecond laser-induced porosity in poly-methyl methacrylate," Appl. Surf. Sci. **282**, 729–734 (2013).
[29]V. V. Zhakhovskil, K. Nishihara, S. I. Anisimov, and N. A. Inogamov, "Molecular-dynamics simulation of rarefaction waves in media that can undergo a phase transition," JETP Lett. **71**, 167–172 (2000).
[30]F. Baset, K. Popov, A. Villafranca, J. M. Guay, Z. A-Rekabi, A. E. Pelling, L. Ramunno, and R. Bhardwaj, "Femtosecond laser-induced surface swelling in poly-methyl methacrylate," Opt. Express **21**, 12527 (2013).
[31]S. Lai, M. Ehrhardt, P. Lorenz, D. Hirsch, J. Zajadacz, J. Lu, B. Han, and K. Zimmer, "Submicron bubbles/voids formation in the subsurface region of soda-lime glass by single-pulse fs laser-induced spallation," Appl. Surf. Sci. **502**, 144134 (2019).
[32]S. I. Anisimov, N. A. Inogamov, A. M. Oparin, B. Rethfeld, T. Yabe, M. Ogawa, and V. E. Fortov, "Pulsed laser evaporation: Equation-of-state effects," Appl. Phys. A **69**, 617–620 (1999).
[33]E. G. Gamaly, S. Juodkazis, H. Misawa, B. L. Davies, A. V. Rode, L. Hallo, P. Nicolai, and V. T. Tikhonchuk, "Formation of nano-voids in transparent dielectrics by femtosecond lasers," Curr. Appl. Phys. **8**, 412–415 (2008).
[34]T. Viertel, L. Pabst, M. Olbrich, R. Ebert, A. Horn, and H. Exner, "Generation of nano-voids inside polylactide using femtosecond laser irradiation," Appl. Phys. A **123**, 789 (2017).
[35]M. Asobe, I. Yokohama, T. Kaino, S. Tomaru, and T. Kurihara, "Nonlinear absorption and refraction in an organic dye functionalized main chain polymer waveguide in the 1.5 μm wavelength region," Appl. Phys. Lett. **67**, 891–893 (1995).
[36]M. D. Crisp, N. L. Boling, and G. Dube, "Importance of Fresnel reflections in laser surface damage of transparent dielectrics," Appl. Phys. Lett. **21**, 364–366 (1972).
[37]E. Nichelatti, "Complex refractive index of a slab from reflectance and transmittance: analytical solution," J. Opt. A Pure Appl. Opt. **4**, 400–403 (2002).
[38]H. A. Macleod, *Thin-Film Optical Filters*, 2nd ed. (Adam Hilger, Bristol, 1986), Chap. 2.
[39]R. F. Potter, "Handbook of optical constants of solids," in *Basic Parameters for Measuring Optical Properties*, edited by E. D. Palik (Academic, London, 1985), Chap. 2.
[40]T. Chang, X. Zhang, X. Zhang, and H. L. Cui, "Accurate determination of dielectric permittivity of polymer from 75 GHz to 1.6 THz using both S-parameters and transmission spectroscopy," Appl. Opt. **56**, 3287–3292 (2017).
[41]C. Schnebelin, C. Cassagne, C. B. D. Araujo, and G. Boudebs, "Measurements of the third- and fifth-order optical nonlinearities of water at 532 and 1064 nm using the D4σ method," Opt. Lett. **39**, 5046–5049 (2014).
[42]M. Gu, A. Satija, and R. P. Lucht, "Effects of self-phase modulation (SPM) on femtosecond coherent anti-stoke Raman scattering spectroscopy," Opt. Express **27**, 33954–33966 (2019).
[43]I. W. Hsieh, X. Chen, J. I. Dadap, N. C. Panoiu, and R. M. Osgood Jr., "Ultrafast-pulse self-phase modulation dispersion in Si photonic wire-waveguides," Opt. Express **14**, 12380–12387 (2006).